Langmuir

Article

pubs.acs.org/Langmuir

Adsorption of Dopamine on Rutile TiO_2 (110): A Photoemission and Near-Edge X-ray Absorption Fine Structure Study

Mark J. Jackman,[†] Karen L. Syres,[‡] David J. H. Cant,[†] Samantha J. O. Hardman,[†] and Andrew G. Thomas*[,†]

[†]School of Physics and Astronomy and Photon Science Institute, Alan Turing Building, The University of Manchester, Oxford Road, Manchester M13 9PL, UK

[‡]School of Chemistry, The University of Nottingham, University Park, Nottingham NG7 2RD, UK

Supporting Information

ABSTRACT: Synchrotron radiation photoelectron spectroscopy and near-edge X-ray absorption fine structure (NEXAFS) techniques have been used to study the adsorption of dopamine on a rutile TiO_2 (110) single crystal. Photoemission results suggest that dopamine bonds through the oxygen molecules in a bidentate fashion. From the data, it is ambiguous whether the oxygens bond to the same 5-fold coordinated surface titanium atom or bridges across two, although based on the bonding of pyrocatechol on rutile TiO_2 (110), it is likely that the dopamine bridges two titanium atoms. Using the searchlight effect, the carbon K-edge near-edge X-ray absorption fine structure NEXAFS spectra recorded for dopamine on rutile TiO_2 (110) show the phenyl ring to be oriented at 78° ± 5° from the surface and twisted 11 ± 10° relative to the (001) direction.

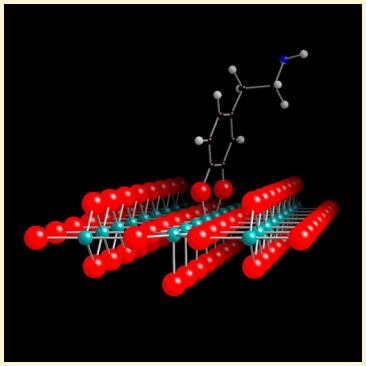

1. INTRODUCTION

TiO_2 is of a significant interest to many applications over a broad range of the technological spectrum. Its use has been investigated for photovoltaics,[1] self-cleaning surfaces,[2] and photocatalysts.[3] The biocompatibility of TiO_2 opens up myriad possibilities within medicinal science such as immunoassays,[4] orthopedic implants,[5] cancer treatment,[6] and drug delivery.[7] TiO_2 is also a promising candidate for a commercial photoelectrode for photoelectrochemical water splitting.[8] It is extremely resistive to corrosion and also photocorrosion in aqueous environments, its properties can be tuned via control of defect chemistry and doping,[9,10] it is an abundant, low-cost material, and it is nontoxic to both humans and the environment. Unfortunately TiO_2 is a large bandgap, n-type semiconductor and only absorbs in the ultraviolet (UV) part of the electromagnetic spectrum. To increase absorption in the peak solar spectrum, organic dyes can be adsorbed on to the surface of TiO_2—an approach that has been utilized in dye-sensitized solar cells[1,11] and water splitting.[12,13]

Dopamine, $C_8H_{11}NO_2$ (Figure 1), is an organic molecule that can modify the surface of TiO_2 and other semiconductors. It can form an anchor, the vicinal diol bonding to the surface (see later) which leaves the terminal amine able to bind to groups such as protoporhphyrins[14] for photodynamic therapy for cancer treatment, and polymers.[15,16] The functionalization of dopamine on TiO_2 nanoparticles has been investigated in solution by Creutz et al.[17] looking to understand the properties of water-soluble Ti(IV) complexes. In common with other catechols, adsorption of dopamine on anatase TiO_2 nanoparticles leads to a shift in the optical absorption onset of the complex. Dopamine functionalization of TiO_2 has been

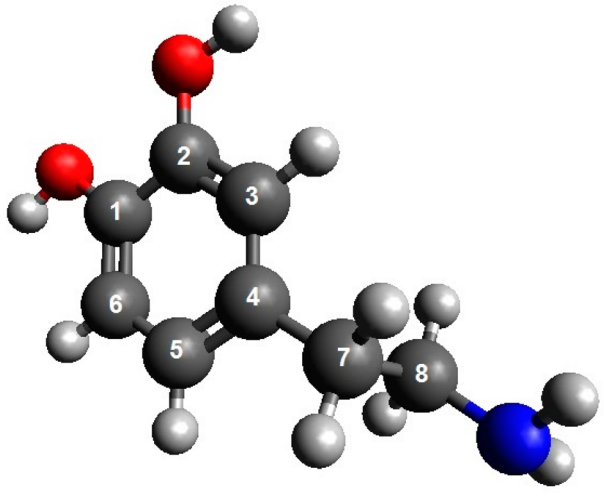

Figure 1. Dopamine molecule (geometry optimized by Gaussian 03[20]). Gray spheres are carbon atoms, the dark blue sphere is the nitrogen atom, the red spheres are the oxygen atoms, and white spheres are hydrogen atoms. The carbon atoms are numbered 1−8 for reference.

Received: April 8, 2014
Revised: May 22, 2014
Published: July 8, 2014

   dx.doi.org/10.1021/la501357b | *Langmuir* 2014, 30, 8761−8769

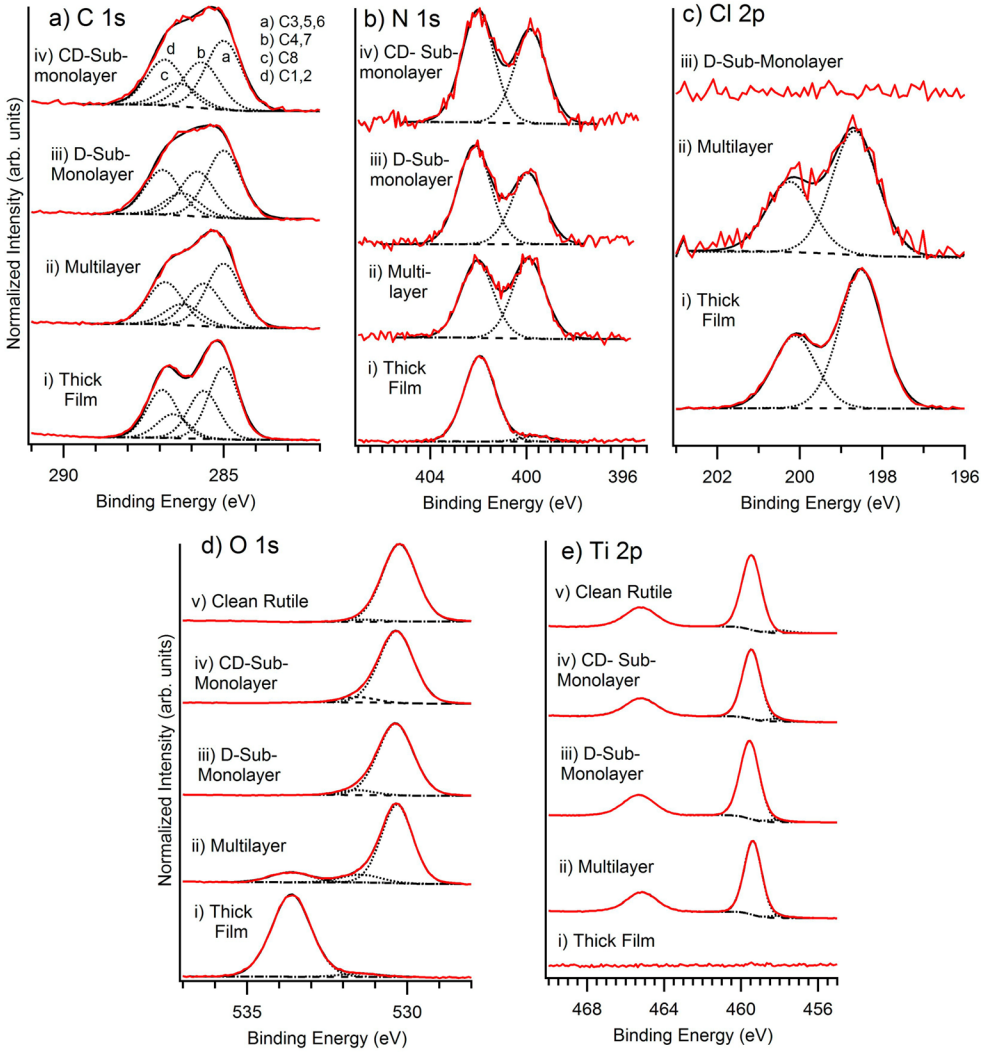

Figure 2. Core XPS spectra for clean rutile TiO_2 (110) (only for Ti and O), submonolayers (D- and CD-method), a multilayer, and a thick film of dopamine adsorbed on rutile TiO_2 (110). The spectra are fitted with a Shirley background (dashed lines) and 70% Gaussian:30% Lorentzian curves curves (dotted lines). See text for a discussion of the results. All spectra were recorded at a photon energy of 1000 eV.

investigated for biomedical applications. For example, PEGylation of anatase nanoparticles has been successfully performed using dopamine as a linker molecule between the nanoparticle and the polymer.[18] PEGylation of titania increases the biocompatibility of the foreign body and the study demonstrates low cytotoxicity of heavily PEGylated nanoparticles. Dopamine has also be used to anchor DNA to TiO_2, thus opening applications in sensing of specific hole-trapping base pairs in DNA.[19]

Studies of the bonding environment of dopamine adsorbed on TiO_2 have been carried out on an anatase TiO_2 (101) single crystal via X-ray photoelectron spectroscopy (XPS), ultraviolet photoelectron spectroscopy (UPS), and near-edge X-ray absorption fine structure spectroscopy (NEXAFS) by Syres et al.[21] Dopamine was found to bond with the phenyl ring normal to the surface. It bonds through the vicinal diols to the 5-coordinated titanium atoms, although the results are ambiguous as to whether the dopamine bonds in a chelating fashion, through both oxygens to a single titanium, or in a bridging fashion to two surface titanium atoms. The study of the simpler pyrocatechol ($C_6H_6O_2$) on single crystal anatase TiO_2 (101)[22] and rutile TiO_2 (110)[22] surfaces yielded similar bonding geometries with the molecule tilted 27° and 23° from the surface normal, respectively. The work by Li et al. examined catechol adsorption to rutile TiO_2 (110) using scanning tunneling microscopy (STM) and photoemission techniques.[23] They found that catechol can bond to the surface in two fashions, either monodentate or mixed mondentate−bidentate, each of which is interconvertible via proton exchange, and that only bidentate bonding results in the formation of bandgap states.

In this paper, core and valence band photoemission results for dopamine adsorbed on single crystal rutile TiO_2 (110) are presented. We determine the orientation of the dopamine molecule on the rutile TiO_2 (110) surface using C K-edge NEXAFS spectroscopy. This work complements that carried out by Syres et al., which details the bonding environment of dopamine on a single crystal of anatase TiO_2 (101),[21] the more photocatalytically active of the TiO_2 polymorphs. An understanding of both polymorphs and the way molecules bond to the surface is imperative in utilizing the correct composite for a particular application.

dx.doi.org/10.1021/la501357b | Langmuir 2014, 30, 8761−8769

Table 1. Binding Energies, Relative Abundances as a Percentage of Total Peak Area, and Assignment of Peaks Fitted to the Core Spectra of a Thick Film, Multilayer, and Submonolayer (Submonolayer Recorded at Grazing Angle) of Dopamine Adsorbed on Rutile TiO_2 (110) via the D-Method, and a Submonolayer Adsorbed on Rutile TiO_2 (110) via the CD-Method[a]

	thick film		multilayer		D-submonolayer (grazing angle emission)		CD-submonolayer	
assignment	BE (eV)	%	BE (eV)	%	BE (eV)	%	BE (eV)	%
C atoms 3, 5, 6 in Figure 1[1,2] (C 1s)	284.5	37.5	284.5	37.5	284.5	37.5	284.5	37.5
C atoms 4, 7 in Figure 1[2] (C 1s)	285.1	25	285.1	25	285.3	25	285.2	25
C atom 8 in Figure 1[2] (C 1s)	286.1	12.5	285.8	12.5	285.8	12.5	285.9	12.5
C atoms 1, 2 in Figure 1[21,22] (C 1s)	286.4	25	286.3	25	286.4	25	286.3	25
N atom in Figure 1[2] (N 1s)	399.9	5.9	399.8	55.2	399.8	41.9	399.8	45.3
protonated N atom in Figure 1[2] (N 1s)	402.0	94.1	401.9	44.8	401.9	58.1	401.9	54.7
lattice O (O 1s)	ND	ND	530.2	77.0	530.2	93.7	530.2	93.7
deprotonated O^2 and Ti−OH (O 1s)	531.4	3.8	531.3	12.0	531.5	6.3	531.4	6.3
molecular O in OH^2 (O 1s)	533.5	96.2	533.4	11.0	ND	ND	ND	ND
Cl atom from HCl salt (Cl $2p_{3/2}$)	198.0	65.7	197.9	63.6	<2%	<2%	<2%	<2%
Cl atom from HCl salt (Cl $2p_{1/2}$)	199.6	34.3	199.5	36.4	<2%	<2%	<2%	<2%

[a]Binding energies are in eV and are quoted to ±0.1 eV. % indicates relative intensity. ND indicats nondetected.

Table 2. Stoichiometry of Thick Film, Multilayer, and Submonolayer of Dopamine on Rutile TiO_2 (110) Surface via the D-Method and Submonolayer via CD-Method (Error: ±0.2)[a]

atom (ref Figure 1)	BE (eV) (thick film)	thick film	multilayer	D-submonolayer (grazing θ)	CD-submonolayer	expected stoichiometry
C3,5,6	284.5	3.0	3.0	3.0	3.0	3.0
C4, 7	285.1	2.0	2.0	2.0	2.0	2.0
C8	286.1	1.0	1.0	1.0	1.0	1.0
C1,2	286.4	2.0	2.0	2.0	2.0	2.0
N1	399.4	0.1	0.4	0.4	0.5	1.0
N2	401.8	0.9	0.4	0.6	0.6	
O1	531.0	0.1	0.8	1.8	2.8	2.0
O2	533.1	1.5	0.9			
Cl	198.0	0.7	0.1	<2%	<2%	see text
	199.6	0.4	0.1			

[a]The stoichiometry of the dopamine on the rutile TiO_2 (110) surface was calculated by dividing the area of the peak by the number of scans and then normalizing for the elemental cross section, as determined by Yeh and Lindau[26] and the transmission functions for the Scienta analyzer with 1.6 mm slits.[27]

2. METHODS

The work was carried out on D1011 ($30 \leq h\nu \leq 1600$ eV), a bending magnet soft X-ray beamline at MAX-lab in Sweden. The D1011 endstation is equipped with a Scienta SES200 200 mm mean-radius hemispherical electron energy analyzer, a microchannel plate (MCP) NEXAFS detector, a low-energy electron diffraction (LEED) camera, and a residual gas analyzer (RGA). The analysis chamber is separated from the sample preparation chamber by means of a gate valve. The rutile TiO_2 (110) crystal (10 mm × 10 mm, Pikem) was held in place by two strips of tantalum wire. A thermocouple was attached to the sample plate, as close to the crystal as possible, allowing the sample temperature to be monitored during the experiment. The crystal was cleaned by repeated 1 keV Ar^+ ion bombardment and annealing to 700 °C in a vacuum until a sharp (1 × 1) LEED pattern was obtained, and the X-ray photoelectron spectrum (XPS) was free from peaks due to contaminants such as C, K, Ca, and Si (see Supporting Information Figure S.1). The base pressure in the analysis chamber was around 1.5×10^{-10} mbar throughout the measurements.

Dopamine hydrochloride (Sigma-Aldrich; purity: 99.5%), a white powder, was thoroughly degassed prior to use by gently heating in a glass dosing tube and venting to waste. To evaporate the dopamine hydrochloride into the vacuum chamber, the dosing tube and the line to the prep chamber were heated to approximately 50 °C. Dosing was carried out via a leak valve. Two methods of preparing a dopamine film were employed:

(1) The desorption method (D-method): A thick film of dopamine hydrochloride was evaporated on to the rutile TiO_2 (110) crystal by dosing at 3×10^{-7} mbar for 10 min (equivalent to ∼140 langmuirs, where 1 langmuir = 1.3×10^{-6} mbar s). The film was deemed thick enough when no substrate photoemission peaks were visible. The RGA confirmed there was no degradation of the dopamine. Next, a multilayer was produced by heating the thick film via the sample plate, desorbing the dopamine until Ti 2p peaks were visible in the photoelectron spectrum. A submonolayer was produced by heating the multilayer until the dopamine molcule exhibited a single O 1s species attribututed to the deprotonated oxygen of the dopamine molecule bonding to the surface.[22]

(2) The controlled-dose method (CD-method): A submonolayer was also formed via a controlled dosing of the crystal at 5×10^{-8} mbar for 12 min (equivalent to ∼28 langmuirs, where 1 langmuir = 1.3×10^{-6} mbar s). We believe a submonolayer was formed and not a monolayer by comparison with catechol on rutile TiO_2 (110) which saturates at monolayer coverage on both anatase and rutile TiO_2 surfaces.[22]

Photoemission spectra were recorded at normal emission. Core level spectra were recorded at 1000 eV photon energy ($h\nu$) and valence band spectra with $h\nu$ = 110 eV. All binding energies (BE) (quoted to ±0.1 eV) are aligned with respect to the aromatic C peaks in the C 1s spectrum of the adsorbed dopamine at 284.5 eV.[21] A Shirley background was subtracted from the data and 70% Gaussian:30% Lorentzian curves were used to fit the core level spectra (with CASA XPS), consistent with previous work on these types of system.[21] NEXAFS spectra were recorded at incident photon angles of $30° \leq \theta \leq 90°$ relative to the surface with the electric vector of the light at 4° relative to the [1$\bar{1}$0] azimuth. The NEXAFS spectra were recorded over the C K-edge using Auger yield via the Scienta

dx.doi.org/10.1021/la501357b | Langmuir 2014, 30, 8761−8769

analyzer with a fixed kinetic energy of 260 eV. Photoemission and NEXAFS spectra were recorded with the sample at room temperature.

Computer modeling was carried out using Gaussian '03[20] and StoBe-deMon.[24] Gaussian '03 was used to perform geometry optimizations of the isolated dopamine molecule. StoBe-deMon software was used to perform density of states and partial density of states calculation for the dopamine molecule.

3. RESULTS AND DISCUSSION

3.1. X-ray Photoelectron Spectroscopy. As described above, two methods were employed to produce a submonolayer of dopamine on the rutile TiO_2 (110) surface: A thick film was produced, and the sample heated so that dopamine was desorbed from the surface to eventually leave a submonolayer (D-method). Photoemission spectra were taken at the following points: (a) the clean rutile TiO_2 (110) surface; (b) following adsorption of a thick film of dopamine; (c) after heating, when a multilayer remained on the surface; (d) after further heating when a submonolayer remained on the surface. In addition, rutile TiO_2 (110) was subjected to a controlled dose of dopamine (CD-method). Photoemission spectra were taken of the clean rutile TiO_2 (110) surface and again following adsorption of a submonolayer of dopamine. Both results will be discussed in unison as both methods result in submonolayer formation.

Figure 2 shows the photoelectron spectra for the thick film, multilayer, D-method submonolayer, CD-method submonolayer, and clean rutile TiO_2 (110). Table 1 shows the binding energies, assignments, and peak ratios. Table 2 shows the stoichiometries of the dopamine molecule on the surface.

Figure 2 a shows the C 1s spectrum. For all the spectra, four peaks have been fitted with a fixed full width half-maximum (fwhm) and a fixed stoichiometric ratio of 3:2:2:1, as expected for this molecule, which has carbon in four different chemical environments, summarized, along with the relative intensities in Tables 1 and 2. Syres et al. fitted two peaks to the C 1s spectrum of dopamine TiO_2 on anatase (101)[21] which yielded a very similar C 1s spectrum, as expected. However, assigning the fitted peaks to individual C atoms results in a good fit, and the binding energies agree with fits to C 1s spectra for similar molecules.[22,25] The thick film C 1s spectrum (Figure 2 a(i)) exhibits a slightly different peak shape that is assigned to a small shift in the binding energy of C8. In the thick film C8 is predominantly bonded to NH_3^+, whereas in the submonolayer and multilayer it is bonded to a mixture of NH_2/NH_3^+, as a result of differing amounts of the HCl salt present in the thick film, the multilayer and the monolayer (as discussed later).

Figure 2b shows the N 1s spectra and Figure 2c the Cl 2p spectrum. Synthetically, dopamine is isolated as an HCl salt (R-ammonium cation and chloride anion). The N 1s spectrum for the thick film (Figure 2b(i)) is predominantly $R-NH_3^+$ with a small contribution from $R-NH_2$. The Cl 2p spectrum (Figure 2c(i)) shows the Cl $2p_{3/2}$ and Cl $2p_{1/2}$ peak split in a 2:1 ratio and a splitting of ∼1.6 eV as expected.[28] Table 2 shows that N and Cl are present in a stoichiometric ratio (1.0:1.1) meaning that the thick film is predominantly the dopamine hydrochloride salt. After heating, when a multilayer is left on the surface (Figure 2b(ii)), the ratio of $R-NH_3^+$:$R-NH_2$ changes to 45:55 and the stoichiometry of N:Cl is reduced to 0.8:0.2. The concentration of N is still in reasonable agreement with the stoichiometry of the molecule (Table 2). This means that Cl^- is desorbed from the surface more readily than the dopamine molecule. After further heating, dopamine is left on the surface as a submonolayer (Figure 2b(iii)). The ratio of the N 1s spectrum (Figure 2b(iii)) for NH_3^+:NH_2 is 58:42, similar to that of the CD-submonolayer: 55:45 (Figure 2b(iv)). Cl is not detected on the surface of the CD-submonolayer (the Cl 2p spectrum was not recorded but Cl 2p was not detected in the wide scan: see Supporting Information Figure S.1) or the D-method submonolayer (Figure 2c(iii)). The limit of detection for photoemission is around 1 at. %; thus, we are unable to definitively rule out the presence of Cl at the surface. Cl 2p was also not observed in the wide scan following adsorption of 1 monolayer of dopamine on the anatase TiO_2 (101) surface.[29] In both cases one would expect to be able to resolve a feature in the wide scan of roughly half the intensity of the peak seen in the multilayer (equivalent to 4% HCl in the film), which means we can rule out a Cl composition of greater than 2%. For dopamine adsorbed on to anatase TiO_2 (101) the ratio of NH_3^+:NH_2 was 49:51.[21] The protonation of the amine group in amino acids bonded to TiO_2 has been well documented.[30−32] Amines bonded to a TiO_2 surface via the nitrogen do not show this higher binding energy peak.[33−35] For dopamine to bond via the oxygen species to TiO_2, one or both protons will dissociate from the diol, and these could be available for bonding to the nitrogen as seen in the zwitterionic amino acids,[25,32] although the mechanism behind this is not clear. What is more likely is that the chloride ion, rather than the HCl, is lost from dopamine-HCl upon heating and a proportion of the nitrogen remains protonated as NH_3^+.

The O 1s spectra, recorded following deposition of dopamine on the rutile TiO_2 (110) surface, are shown in Figure 2d. The thick film O 1s spectrum (Figure 2d(i)) contains two oxygen species. The peak at higher binding energy (533.5 eV) is attributed to the intact molecular hydroxyls attached to C1 and C2 in the dopamine molecule; i.e., they remain protonated in the thick film. The peak at a binding energy of 531.4 eV most probably arises from a small number of deprotonated diols, which are available to protonate the amine group. The binding energy is also in agreement with Ti-surface hydroxyls, but since the substrate O 1s cannot be observed at this film thickness, this is unlikely. After heating, to produce a multilayer on the surface (Figure 2d(ii)), the TiO_2 substrate O 1s peak becomes evident at a binding energy of 530.2 eV. The desorption of dopamine leads to a decrease in the intensity of the peak at 533.4 eV, attributed to intact hydroxyls in the dopamine molecule. The peak at 531.4 eV also increases in relative intensity due to the deprotonated oxygen atoms of the first monolayer of the dopamine molecule becoming detectable through partial removal of the thick film. The relative intensity of the intact dopamine hydroxyls and the surface-bound dopamine oxygen molecules is approximately equal (0.8:0.9). The nature of the multilayer cannot be determined from the data here. It is possible that there are two layers: one bound to the surface, with a second layer of dopamine physisorbed or hydrogen bonded through an amine−diol interaction. However, the data are also consistent with the formation of multilayer islands as the molecule is desorbed. The difficulty in forming a monolayer of dopamine on this surface by either the CD-dosed or D-method would support adsorption and desorption following an island growth mechanism.

Further heating results in the formation of a submonolayer (Figure 2d(iii)) where the O 1s peak at a binding energy of 533.4 eV is completely removed, thus indicating that all dopamine hydroxyls in this layer have dissociated. The ratio of

dx.doi.org/10.1021/la501357b | Langmuir 2014, 30, 8761−8769

the oxygen to carbon in the molecule is in good agreement with the expected stoichiometry (1.0:1.8). The CD-dosed submonolayer has a high O stoichiometry (2.8). This is possibly due to the CD method resulting in some contamination by Ti−OH, whereas these would have been removed by the heating in the D-method submonolayer. With the data presented here, the precise nature of the bonding of the dopamine to the rutile surface is not certain. Whereas we can say that there are no intact dopamine hydroxyls in the submonolayers, which indicates that dopamine bonds in a bidentate fashion, we cannot say whether the dopamine bonds to the titanium in a bridging or a chelating fashion. The same conclusions were drawn for pyrocatechol on TiO_2[22] and dopamine on anatase TiO_2 (101).[21] However, DFT calculations of catechol on rutile TiO_2 (110) carried out by Li et al.[23] show that the most energetically favorable bonding environment is the vicinal diols bonding to two titanium atoms in a bridging fashion, and we believe that to be the case with dopamine on rutile TiO_2 (110). Li et al. observed proton transfer between the surface and bound catechol reforming the molecular hydroxyl groups.[23] However, no intact hydroxyls were observed on either the D-dosed or CD-dosed submonolayers, studied in the present work, in agreement with simple carboxylic adsorption in UHV on vacuum-prepared rutile TiO_2 surfaces.[36,37]

The Ti 2p spectra in Figure 2e show the clean Ti 2p spectrum (Figure 2e(v)) consists of the spin−orbit-split Ti $2p_{3/2}$ and Ti $2p_{1/2}$.[38] Peak fitting is only carried out on the Ti $2p_{3/2}$, which has a binding energy of 459.0 eV. There is some evidence of residual Ti^{3+}[39] at 457.6 eV BE (4% of the peak area) which is attributed to residual surface oxygen vacancies[40] or subsurface oxygen vacancies.[41] Since each O-vacancy results in the formation of two surface Ti^{3+} species, we estimate an O-vacancy concentration of around 2% on the surfaces studied here.[42] This low vacancy concentration is further supported by the valence band spectra discussed below, where we see very little intensity in the band gap state at 1 eV below E_F.[40] Upon absorption of dopamine there is a very small decrease in the relative intensity of the Ti^{3+} peak from 4% to 3% (Figure 2e(ii−iv)). The change in Ti^{3+} concentration will be considered further in the valence band analysis below.

3.2. UV Photoelectron Spectroscopy. Figure 3 shows partial density of states simulations for carbon, nitrogen, and oxygen atoms. The partial density of states simulations show the contributions of the different atoms in the dopamine molecule to the total density of states simulation. It is obvious that the carbon atoms contribute most to the total density of states simulation. The total DOS was calculated using the coordinates of the optimized dopamine molecule from Gaussian with triple zeta and valence polarization (TZVP) basis sets for the calculation. The HOMO at approximately 5.7 eV binding energy has contributions from carbon, oxygen, and nitrogen atoms. This is supported by a molecular orbital calculation of the HOMO on the dopamine molecule (see Figure 3). As mentioned above, it can be seen that the HOMO is mainly associated with the π-system of the molecule.

Figure 4 shows a comparison of the DFT calculated total density of states spectrum of dopamine generated using StoBe (Figure 4a) with a thick film of dopamine (Figure 4b) and the difference spectrum (Figure 4c) of the submonolayer-dosed spectrum (Figure 4d) and the clean rutile TiO_2 (110) spectrum (Figure 4e). The StoBe-calculated spectrum is shifted by 2.9 eV to lower binding energy to align with the experimental difference spectrum (for dopamine adsorbed on to anatase

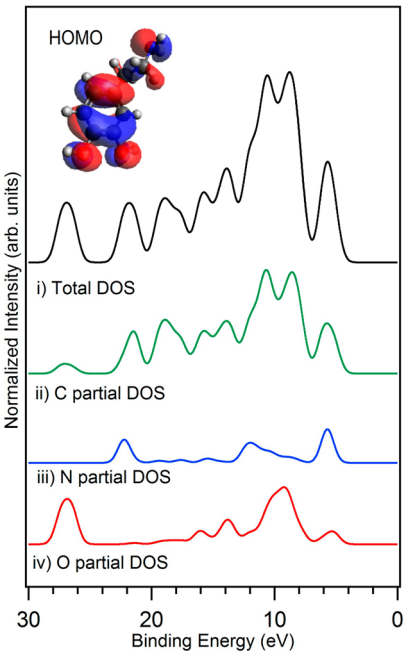

Figure 3. StoBe-calculated partial density of states (DOS) of carbon (green), nitrogen (blue), and oxygen atoms (red) in the dopamine free molecule and the total density of states they generate (black). Top left is the HOMO of dopamine, calculated by Gaussian.[20]

TiO_2 (101) the shift was 3.2 eV[29]). This accounts for the relaxation/polarization shift upon adsorption, i.e., the binding energy difference between that of the gas phase molecule (in this case the calculation) and that of the adsorbed molecule. This shift occurs because the final state in photoemission from the adsorbed molecule is screened by the presence of the surface.[43] The features in the difference spectrum and the thick film agree reasonably well with the calculation.

The valence band spectrum for clean rutile TiO_2 (110) is shown in Figure 4e. The spectrum was recorded at 110 eV photon energy and aligned on the binding energy scale using the binding energy of the band gap state at 1.0 eV.[42] The mainly O 2p derived valence band for the rutile TiO_2 (110) surface has peaks at 6.4 and 7.1 eV BE, which is consistent with previous work.[42] The clean rutile TiO_2 (110) spectrum exhibits a very weak band gap state at 1.0 eV BE, indicating the presence of surface defects in the form of O-vacancies.[25] This defect peak has been ascribed to occupation of Ti 3d states after Ti^{3+} (d^1) is created at the surface due to oxygen vacancies.[40,44] The presence and low intensity of this defect state correlates with the Ti 2p spectrum (Figure 2d) where a weak signal due to Ti^{3+} was also observed. Figure 4d shows the valence band spectrum following adsorption of a submonolayer of dopamine on the rutile TiO_2 (110) surface (using the CD-method) recorded at 110 eV, and the difference spectrum (Figure 4c) is obtained by subtracting the clean rutile TiO_2 (110) spectrum (Figure 4e) from the dopamine-dosed rutile TiO_2 (110) spectrum (Figure 4d). Adsorption of dopamine leads to a number of new peaks, attributed to the valence states and shallow core levels of the absorbate, appearing in the spectrum at 2.8, 5.8, 8.3, 11.0, 13.6, 15.8, and 17.4 eV. The defect feature at 1.0 eV binding energy observed in the spectrum recorded from the clean rutile surface remains relatively unchanged following adsorption of dopamine. However, a spectrum recorded at a photon energy of 47 eV (see inset, Figure 4), corresponding to the Ti 3p to 3d

dx.doi.org/10.1021/la501357b | Langmuir 2014, 30, 8761−8769

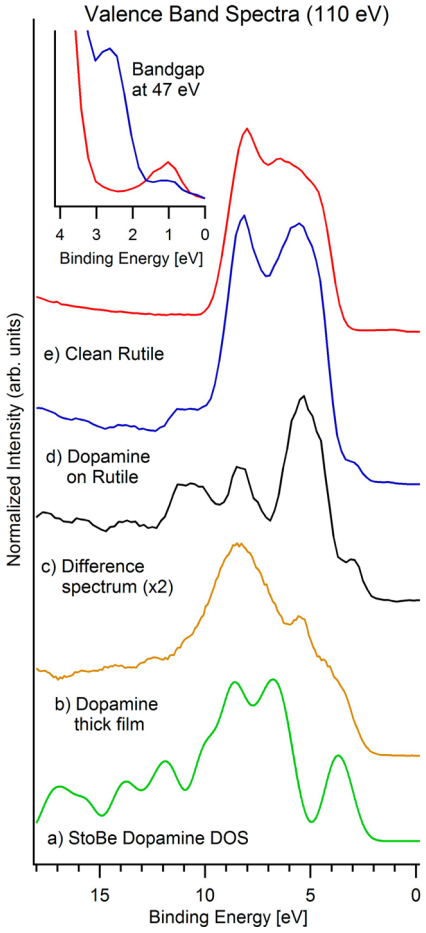

Figure 4. Comparison of the StoBe-calculated total density of states (a, green) with valence band spectra recorded at photon energy 110 eV for a thick film of dopamine (b, orange), the difference spectrum (c, black) of a submonolayer of dopamine adsorbed on rutile TiO_2 (110) (d, blue), and clean rutile TiO_2 (110 surface) (e, red). The inset graph shows the bandgap state region for clean rutile TiO_2 (red) and a submonolayer of dopamine dosed on rutile TiO_2 at 47 eV (on resonance) (blue).

resonance which can be considered as a probe of Ti 3d character, shows a marked decrease in the intensity of the state following adsorption of dopamine.[45] This decrease is also in agreement with that observed in the Ti 2p spectra above. The decrease in intensity could be attributed to a reduction in oxygen vacancies on adsorption of dopamine, an effect which was also observed following dopamine adsorption on anatase TiO_2 (101).[21] Another possibility is that the Ti^{3+} is attenuated upon adsorption of dopamine in relation to Ti^{4+} due to preferred adsorption at such sites. For clean rutile TiO_2 (110) the valence band maximum (VBM) is located at 2.9 eV below the Fermi level (E_F), but upon adsorption of a submonolayer of dopamine a shoulder is observed on the low binding energy side of the TiO_2 VB with a cutoff at 2.0 eV. This shoulder is attributed to the highest occupied molecular orbital (HOMO) of the dopamine molecule arising from π-states in the phenyl ring system as discussed below. Its position and energy are in good agreement with adsorption studies of dopamine on anatase TiO_2 (101)[21] and catechol on rutile TiO_2 (110) and anatase TiO_2 (101) surfaces.[22] The position of the HOMO matches well with the optical band gap of dopamine adsorbed on TiO_2 of 1.9 eV (dopamine on TiO_2 nanoparticles).[46] Dopamine absorption therefore leads to TiO_2 adsorbing in the visible spectrum in agreement with UV−vis absorption studies.[17] The difference spectrum is in good agreement between the calculated density of states spectrum of the free dopamine molecule and the experimental difference spectrum at the valence band maximum. However, as expected, there are differences in the deeper parts of the valence band region, presumably due to deprotonation of the dopamine molecule upon adsorption.

3.3. Near-Edge X-ray Absorption Spectroscopy. Figure 5a shows the carbon K-edge NEXAFS spectra of a submonolayer of dopamine adsorbed on rutile TiO_2 (110) for incident radiation angles of 30°−90° to the surface. The spectra are first normalized, in order to remove photon flux and substrate-induced features, by dividing the dopamine-dosed rutile TiO_2 (110) carbon K-edge NEXAFS spectrum by the corresponding clean rutile TiO_2 (110) spectrum. The resulting spectra are further normalized by setting the height of the step edge (the increase in intensity when passing the ionization potential) to unity. Sharp shape resonances due to C 1s → π^* excitations are seen at photon energies below 288 eV. These peaks are assigned as follows: the peak at 284.5 eV photon energy (peak A) in Figure 5a arises from excitations from the C 1s level into the π^* orbitals of carbon atoms 3−6 (C−C/C−H).[47] The peak at 285.9 eV (peak B) originates from C 1s → π^* excitations for carbon atoms 1, 2 (C−O).[21] The peaks have a height ratio of approximately 2:1 as expected. Both peaks exhibit a degree of asymmetry which is due to excitation from the chemically shifted C 1s states into the π^*-derived lowest unoccupied molecular orbital (LUMO) and LUMO+1 states. Figure 5b shows the detail in the NEXAFS spectrum at normal incidence as well as the first two LUMOs, as calculated by Gaussian 03.[20] Figure 5c shows the different NEXAFS spectra normalized to the intensity of peak a, recorded at normal incidence. Stöhr[48] equations were fitted to the data points (Figure 5c). The fit gives an angle for the π^* vector-like orbital almost parallel to the surface (i.e., the molecule is oriented with the plane of the phenyl ring oriented 78 ± 5° away from the surface) and twisted roughly 11 ± 10° from the (001) azimuth (Figure 5d). This fits quite well with DFT calculations performed by Castillo et al., who determined dopamine to sit approximately normal to the surface,[49] although the calculations were based around an intact dopamine molecule adsorbing on the surface, without deprotonation. Experimental NEXAFS analysis of dopamine on anatase TiO_2 (101) showed that it adsorbs in an almost upright geometry, i.e., with the plane of the ring at around 90° the surface which, given experimental error is reasonably similar. Catechol adsorbed on rutile TiO_2 (110) bonds with the benzene ring parallel to the (001) azimuth[23] and at 67° away from the surface.[22] The slight difference in the tilt angle of the molecule between anatase and rutile may lie in the coverage. In the work of Syres et al. studying the adsorption of dopamine on anatase TiO_2 (101) the coverage was estimated as a monolayer, whereas here submonolayer coverage is studied. This means in the present case steric effects will be reduced which may allow the molecules to tilt away from the normal. This coverage-dependent orientation behavior has been observed for a number of systems.[48]

4. CONCLUSIONS

Dopamine was found to adsorb dissociatively on the rutile TiO_2 (110) surface following deprotonation of the alcohol groups.

dx.doi.org/10.1021/la501357b | Langmuir 2014, 30, 8761−8769

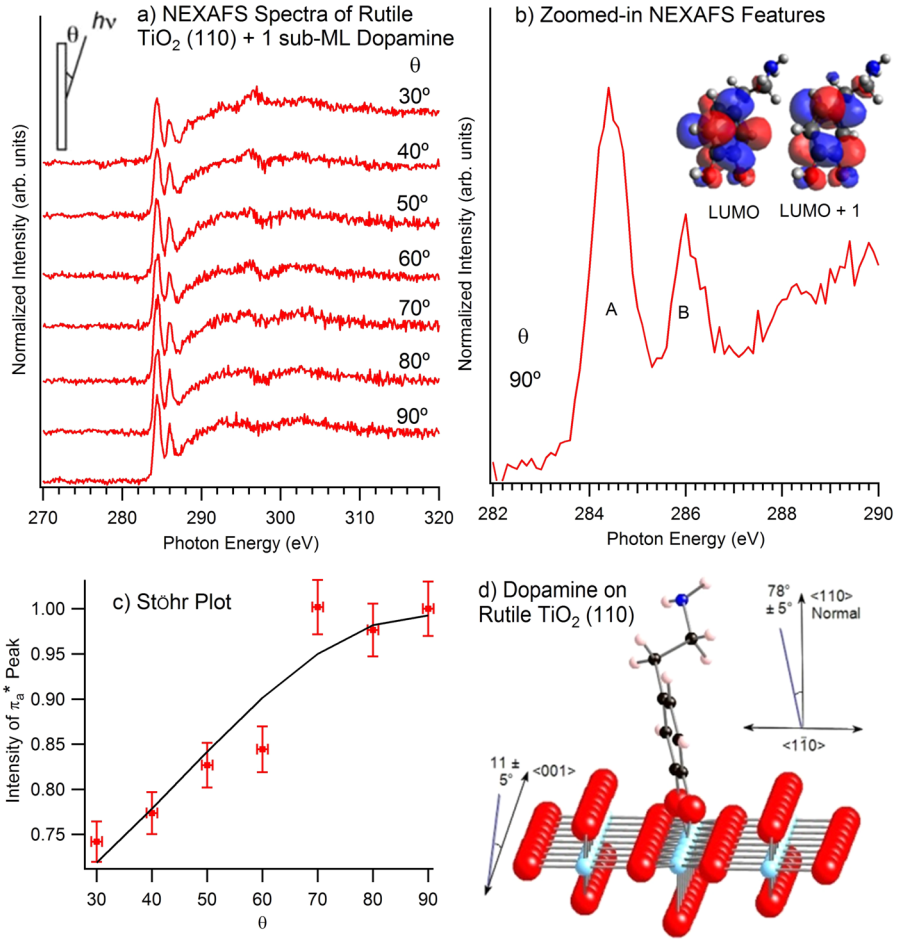

Figure 5. (a) Carbon K-edge NEXAFS spectra of dopamine adsorbed on rutile TiO_2 (110) surface. (b) shows the resulting height of the π_a* peaks plotted as a function of angle of photon incidence to the surface, with the Stöhr equations[48] fitted to the data points. (c) Zoomed-in view of carbon K-edge NEXAFS spectra of dopamine adsorbed on rutile TiO_2 (110) surface at normal incidence. Peak A corresponds to carbons 3−6 of Figure 1 (C−H) and peak B to carbons 1, 2 (C−O). Multiple components are likely to be present which correspond to transitions to the lowest unoccupied molecular orbitals, displayed inset (calculated by Gaussian 03[20]). (d) A dopamine molecule adsorbed on an rutile TiO_2 (110) cluster. Titanium is represented by light blue, oxygen by red atoms, carbon atoms by gray, and hydrogens by white.

The data suggest bonding occurs through the dopamine oxygen atoms in a bidentate fashion to the 5-fold-coordinated Ti atoms at the TiO_2 (110) surface. Although the data cannot unambiguously distinguish between a chelating (both oxygen atoms bonding to a single 5-fold-coordinated surface Ti) and a bridging (oxygens bonded to neighboring surface Ti) by analogy with studies of catechol[23] and carboxylic acids,[37] we conclude that the bridging mode would appear more likely. Angle-resolved NEXAFS spectra show the plane of the ring of the molecule to be tilted 78 ± 5° away from the surface (i.e., the molecule is almost upright on the surface) and twisted roughly 11 ± 5° off the (001) direction. The difference in tilt angle with regard to the adsorption of dopamine on the anatase TiO_2(101) surface is attributed to the lower coverage on the rutile surface leading to a reduction in steric repulsion between the adsorbate molecules.

■ ASSOCIATED CONTENT

Supporting Information

Figure of the wide scan for clean rutile TiO_2 (110) and a submonolayer dosed on rutile TiO_2 (110). This material is available free of charge via the Internet at http://pubs.acs.org.

■ AUTHOR INFORMATION

Corresponding Author

*E-mail: a.g.thomas@manchester.ac.uk (A.G.T.).

Present Address

S.J.O.H.: Manchester Institute of Biotechnology, The University of Manchester, 131 Princess Street, Manchester M1 7DN, UK.

Notes

The authors declare no competing financial interest.

■ ACKNOWLEDGMENTS

The authors thank MAX-lab for the award of experimental beam time funded by the Swedish Research Council and The European Community's Seventh Framework Programme (FP7/2007-2013) under grant agreement no. 226716. M.J.J. and D.J.H.C. thank EPSRC (UK) for the award of studentships through the NowNano Doctoral Training Centre (grant EP/G03737X/1). K.L.S. thanks EPSRC (UK) for a studentship. S.J.O.H. was funded by EPSRC grant no. EP/E036287/1. A.T. thanks the Photon Science Institute and The University of Manchester for funding. The authors are grateful to Alexei Preobrajenski for training and technical advice on use of the beamline.

■ ABBREVIATIONS

NEXAFS, near-edge X-ray absorption fine structure; LEED, low-energy electron diffraction; XPS, X-ray photoelectron spectroscopy; UPS, ultraviolet photoelectron spectroscopy; CD, controlled dose; D, desorption; HOMO, highest occupied molecular orbital; LUMO, lowest unoccupied molecular orbital; VBM, valence band maximum.

■ REFERENCES

(1) Gratzel, M. Dye-Sensitized Solar Cells. *J. Photochem. Photobiol., C* **2003**, *4*, 145−153.

(2) Mu, Q. H.; Li, Y. G.; Wang, H. Z.; Zhang, Q. H. Self-Organized TiO_2 Nanorod Arrays on Glass Substrate for Self-Cleaning Antireflection Coatings. *J. Colloid Interface Sci.* **2012**, *365*, 308−313.

(3) Henderson, M. A. A Surface Science Perspective on TiO_2 Photocatalysis. *Surf. Sci. Rep.* **2011**, *66*, 185−297.

(4) He, R.; Zhao, L.; Liu, Y.; Zhang, N.; Cheng, B.; He, Z.; Cai, B.; Li, S.; Liu, W.; Guo, S.; et al. Biocompatible TiO_2 Nanoparticle-Based Cell Immunoassay for Circulating Tumor Cells Capture and Identification from Cancer Patients. *Biomed. Microdevices* **2013**, *15*, 617−626.

(5) Kummer, K. M.; Taylor, E.; Webster, T. J. Biological Applications of Anodized TiO_2 Nanostructures: A Review from Orthopedic to Stent Applications. *Nanosci. Nanotechnol. Lett.* **2012**, *4*, 483−493.

(6) Kalbacova, M.; Macak, J. M.; Schmidt-Stein, F.; Mierke, C. T.; Schmuki, P. TiO_2 Nanotubes: Photocatalyst for Cancer Cell Killing. *Phys. Status Solidi RRL* **2008**, *2*, 194−196.

(7) Li, H.; Ma, T.-Y.; Kong, D.-M.; Yuan, Z.-Y. Mesoporous Phosphonate-TiO_2 Nanoparticles for Simultaneous Bioresponsive Sensing and Controlled Drug Release. *Analyst* **2013**, *138*, 1084−1090.

(8) Gratzel, M. Photoelectrochemical Cells. *Nature* **2001**, *414*, 338−344.

(9) Naldoni, A.; Allieta, M.; Santangelo, S.; Marelli, M.; Fabbri, F.; Cappelli, S.; Bianchi, C. L.; Psaro, R.; Dal Santo, V. Effect of Nature and Location of Defects on Bandgap Narrowing in Black TiO_2 Nanoparticles. *J. Am. Chem. Soc.* **2012**, *134*, 7600−7603.

(10) Aschauer, U.; He, Y.; Cheng, H.; Li, S.; Diebold, U.; Selloni, A. Influence of Subsurface Defects on the Surface Reactivity of TiO_2. *Water on Anatase (101)* **2010**, 1278−1284.

(11) Hagfeldt, A.; Boschloo, G.; Sun, L.; Kloo, L.; Pettersson, H. Dye-Sensitized Solar Cells. *Chem. Rev.* **2010**, *110*, 6595−6663.

(12) Youngblood, W. J.; Lee, S.-H. A.; Maeda, K.; Mallouk, T. E. Visible Light Water Splitting Using Dye-Sensitized Oxide Semiconductors. *Acc. Chem. Res.* **2009**, *42*, 1966−1973.

(13) Youngblood, W. J.; Lee, S. H. A.; Kobayashi, Y.; Hernandez-Pagan, E. A.; Hoertz, P. G.; Moore, T. A.; Moore, A. L.; Gust, D.; Mallouk, T. E. Photoassisted Overall Water Splitting in a Visible Light-Absorbing Dye-Sensitized Photoelectrochemical Cell. *J. Am. Chem. Soc.* **2009**, *131*, 926−927.

(14) Kemikli, N.; Kavas, H.; Kazan, S.; Baykal, A.; Ozturk, R. Synthesis of Protoporphyrin Coated Superparamagnetic Iron Oxide Nanoparticles via Dopamine Anchor. *J. Alloys Compd.* **2010**, *502*, 439−444.

(15) Yah, W. O.; Xu, H.; Soejima, H.; Ma, W.; Lvov, Y.; Takahara, A. Biomimetic Dopamine Derivative for Selective Polymer Modification of Halloysite Nanotube Lumen. *J. Am. Chem. Soc.* **2012**, *134*, 12134−12137.

(16) Oschmann, B.; Bresser, D.; Tahir, M. N.; Fischer, K.; Tremel, W.; Passerini, S.; Zentel, R. Polyacrylonitrile Block Copolymers for the Preparation of a Thin Carbon Coating around TiO_2 Nanorods for Advanced Lithium-Ion Batteries. *Macromol. Rapid Commun.* **2013**, *34*, 1693−1700.

(17) Creutz, C.; Chou, M. H. Binding of Catechols to Mononuclear Titanium(IV) and to 1- and 5-nm TiO_2 Nanoparticles. *Inorg. Chem.* **2008**, *47*, 3509−3514.

(18) Kotsokechagia, T.; Zaki, N. M.; Syres, K.; de Leonardis, P.; Thomas, A.; Cellesi, F.; Tirelli, N. PEGylation of Nanosubstrates (Titania) with Multifunctional Reagents: At the Crossroads between Nanoparticles and Nanocomposites. *Langmuir* **2012**, *28*, 11490−11501.

(19) Liu, J.; de la Garza, L.; Zhang, L.; Dimitrijevic, N. M.; Zuo, X.; Tiede, D. M.; Rajh, T. Photocatalytic Probing of DNA Sequence by Using TiO_2/Dopamine-DNA Triads. *Chem. Phys.* **2007**, *339*, 154−163.

(20) Frisch, M. J.; Trucks, G. W.; Schlegel, H. B.; Scuseria, G. E.; Robb, M. A.; Cheeseman, J. R.; Montgomery, Jr., J. A.; Vreven, T.; Kudin, K. N.; Burant, J. C.; Millam, J. M.; Iyengar, S. S.; Tomasi, J.; Barone, V.; Mennucci, B.; Cossi, M.; Scalmani, G.; Rega, N.; Peters, G. A.; Gonzalez, C.; Pople, J. A. *GAUSSIAN 03 (Revision B.02)*; Gaussian, Inc.: Wallingford, CT, 2004.

(21) Syres, K.; Thomas, A.; Bondino, F.; Malvestuto, M.; Gratzel, M. Dopamine Adsorption on Anatase TiO_2 (101): A Photoemission and NEXAFS Spectroscopy Study. *Langmuir* **2010**, *26*, 14548−14555.

(22) Syres, K. L.; Thomas, A. G.; Flavell, W. R.; Spencer, B. F.; Bondino, F.; Malvestuto, M.; Preobrajenski, A.; Gratzel, M. Adsorbate-Induced Modification of Surface Electronic Structure: Pyrocatechol Adsorption on the Anatase TiO_2 (101) and Rutile TiO_2 (110) Surfaces. *J. Phys. Chem. C* **2012**, *116*, 23515−23525.

(23) Li, S. C.; Wang, J. G.; Jacobson, P.; Gong, X. Q.; Selloni, A.; Diebold, U. Correlation between Bonding Geometry and Band Gap States at Organic-Inorganic Interfaces: Catechol on Rutile TiO_2 (110). *J. Am. Chem. Soc.* **2009**, *131*, 980−984.

(24) Pettersson, L.; Hermann, K. StoBe-deMon SOFTWARE, Berlin Version 2.2 of deMon, 2006.

(25) Thomas, A. G.; Flavell, W. R.; Chatwin, C. P.; Kumarasinghe, A. R.; Rayner, S. M.; Kirkham, P. F.; Tsoutsou, D.; Johal, T. K.; Patel, S. Adsorption of Phenylalanine on Single Crystal Rutile TiO_2 (110) Surface. *Surf. Sci.* **2007**, *601*, 3828−3832.

(26) Yeh, J. J.; Lindau, I. Atomic Subshell Photoionization Cross-Sections and Asymmetry Parameters - 1 Less-Than-or-Equal-to Z Less-Than-or-Equal-to 103. *At. Data Nucl. Data Tables* **1985**, *32*, 1−155.

(27) Jeong, H. K.; Komesu, T.; Yang, C. S.; Dowben, P. A.; Schultz, B. D.; Palmstrom, C. J. Photoemission Forward Scattering from ErAs(100)/GaAs(100). *Mater. Lett.* **2004**, *58*, 2993−2996.

(28) Yue, J.; Epstein, A. J. XPS Study of Self-Doped Conducting Polyaniline and Parent Systems. *Macromolecules* **1991**, *24*, 4441−4445.

(29) Syres, K. L. Molecular Adsorption on TiO_2 Surfaces Modelling Potential Biomedical and Photovoltaic Devices. A Thesis Submitted to the University of Manchester for the Degree of Doctor of Philosophy in the Faculty of Engineering and Physical Sciences, 2010.

(30) Thomas, A. G.; Flavell, W. R.; Chatwin, C. P.; Kumarasinghe, A. R.; Rayner, S. M.; Kirkham, P. F.; Tsoutsou, D.; Johal, T. K.; Patel, S. Adsorption of Phenylalanine on Single Crystal Rutile TiO_2 (110) Surface. *Surf. Sci.* **2007**, *601*, 3828−3832.

(31) Wilson, J. N.; Dowler, R. M.; Idriss, H. Adsorption and Reaction of Glycine on the Rutile TiO_2 (011) Single Crystal Surface. *Surf. Sci.* **2011**, *605*, 206−213.

(32) Fleming, G. J.; Adib, K.; Rodriguez, J. A.; Barteau, M. A.; White, J. M.; Idriss, H. The Adsorption and Reactions of the Amino Acid Proline on Rutile TiO_2 (010) Surfaces. *Surf. Sci.* **2008**, *602*, 2029−2038.

(33) Jackman, M. J.; Thomas, A. G. Adsorption and Photocatalytic Degradation of 3-Fluoroaniline on Anatase TiO_2 (101): A Photoemission and Near-Edge X-Ray Absorption Fine Structure Study. *J. Phys. Chem. C* **2014**, *118*, 2028−2036.

(34) Farfan-Arribas, E.; Madix, R. J. Characterization of the Acid-Base Properties of the TiO_2 (110) Surface by Adsorption of Amines. *J. Phys. Chem. B* **2003**, *107*, 3225−3233.

(35) Li, S. C.; Diebold, U. Reactivity of TiO_2 Rutile and Anatase Surfaces toward Nitroaromatics. *J. Am. Chem. Soc.* **2010**, *132*, 64−+.

(36) Quah, E. L.; Wilson, J. N.; Idriss, H. Photoreaction of the Rutile TiO_2 (011) Single-Crystal Surface: Reaction with Acetic Acid. *Langmuir* **2010**, *26*, 6411−6417.

(37) Thomas, A. G.; Syres, K. L. Adsorption of Organic Molecules on Rutile TiO_2 and Anatase TiO_2 Single Crystal Surfaces. *Chem. Soc. Rev.* **2012**, *41*, 4207−4217.

(38) Armitage, D. A.; Grant, D. M. Characterisation of Surface-Modified Nickel Titanium Alloys. *Mater. Sci. Eng., A* **2003**, *349*, 89−97.
(39) Bertoti, I.; Mohai, M.; Sullivan, J. L.; Saied, S. O. Surface Characterization of Plasma-Nitrided Titanium - an XPS Study. *Appl. Surf. Sci.* **1995**, *84*, 357−371.
(40) Diebold, U. The Surface Science of Titanium Dioxide. *Surf. Sci. Rep.* **2003**, *48*, 53−229.
(41) Wendt, S.; Sprunger, P. T.; Lira, E.; Madsen, G. K. H.; Li, Z. S.; Hansen, J. O.; Matthiesen, J.; Blekinge-Rasmussen, A.; Laegsgaard, E.; Hammer, B.; et al. The Role of Interstitial Sites in the Ti3d Defect State in the Band Gap of Titania. *Science* **2008**, *320*, 1755−1759.
(42) Thomas, A. G.; Flavell, W. R.; Mallick, A. K.; Kumarasinghe, A. R.; Tsoutsou, D.; Khan, N.; Chatwin, C.; Rayner, S.; Smith, G. C.; Stockbauer, R. L.; et al. Comparison of the Electronic Structure of Anatase and Rutile TiO_2 Single-Crystal Surfaces Using Resonant Photoemission and X-Ray Absorption Spectroscopy. *Phys. Rev. B* **2007**, *75*.
(43) Flavell, W. R.; Laverty, J. H.; Law, D. S. L.; Lindsay, R.; Muryn, C. A.; Flipse, C. F. J.; Raiker, G. N.; Wincott, P. L.; Thornton, G. H_2O Adsorption on $Bi_2Sr_2CaCu_2O_8(001)$. *Phys. Rev. B* **1990**, *41*, 11623−11626.
(44) Thompson, T. L.; Yates, J. T. Surface Science Studies of the Photoactivation of TiO_2 - New Photochemical Processes. *Chem. Rev.* **2006**, *106*, 4428−4453.
(45) Nerlov, J.; Ge, Q. F.; M?ller, P. J. Resonant Photoemission from TiO_2 (110) Surfaces: Implications on Surface Bonding and Hybridization. *Surf. Sci.* **1996**, *348*, 28−38.
(46) Dugandžić, I. M.; Jovanović, D. J.; Mančić, L. T.; Milošević, O. B.; Ahrenkiel, S. P.; Šaponjić, Z. V.; Nedeljković, J. M. Ultrasonic Spray Pyrolysis of Surface Modified TiO_2 Nanoparticles with Dopamine. *Mater. Chem. Phys.* **2013**, *143*, 233−239.
(47) Solomon, J. L.; Madix, R. J.; Stohr, J. Orientation and Absolute Coverage of Benzene, Aniline, and Phenol on Ag(110) Determined by NEXAFS and XPS. *Surf. Sci.* **1991**, *255*, 12−30.
(48) Stöhr, J. *NEXAFS Spectroscopy*; Springer-Verlag: Berlin, 2003.
(49) Castillo, D.; Ontaneda, J.; Stashans, A. Geometry of Dopmaine Adsorption on Rutile (110) Surface. *Int. J. Mod. Phys. B* **2014**, *28*, 1450071.